Water Catalysis and Anticatalysis in Photochemical Reactions: Observation of a Delayed Threshold Effect in the Reaction Quantum Yield

3 AUTHORS, INCLUDING:

Kaito Takahashi
Academia Sinica

43 PUBLICATIONS **542** CITATIONS

Water Catalysis and Anticatalysis in Photochemical Reactions: Observation of a Delayed Threshold Effect in the Reaction Quantum Yield

Zeb C. Kramer,[†,‡] Kaito Takahashi,[†,§] and Rex T. Skodje*,[†,‡]

Department of Chemistry and Biochemistry, University of Colorado, Boulder, Colorado 80309-0215, and Key State Laboratory of Molecular Reaction Dynamics, Dalian Institute of Chemical Physics, CAS, Dalian, China

Received August 15, 2010; E-mail: Rex.Skodje@colorado.edu

Abstract: The possible catalysis of photochemical reactions by water molecules is considered. Using theoretical simulations, we investigate the HF-elimination reaction of fluoromethanol in small water clusters initiated by the overtone excitation of the hydroxyl group. The reaction occurs in competition with the process of water evaporation that dissipates the excitation and quenches the reaction. Although the transition state barrier is stabilized by over 20 kcal/mol through hydrogen bonding with water, the quantum yield versus energy shows a pronounced delayed threshold that effectively eliminates the catalytic effect. It is concluded that the quantum chemistry calculations of barrier lowering are not sufficient to infer water catalysis in some photochemical reactions, which instead require dynamical modeling.

It is well appreciated that water molecules will catalyze certain neutral chemical reactions so that their rates in solution are substantially higher than those in the gas phase. Such enhancements have been observed experimentally or observed in large theoretical simulations for a variety of reactions including Diels−Alder, dehalogenation, dehydration, and decarboxylation reactions.[1−11] M. Eigen,[12] R. P. Bell,[13] and others[14] conjectured long ago that water molecules may participate in an essential way in H-atom (or proton) transfer reactions by forming hydrogen bonded complexes at the transition state (TS). Using finite clusters of reagent and water molecules, quantum chemistry calculations[15] have confirmed that the TS energy for a variety of reactions can be significantly lowered compared to the bare (i.e., nonhydrated) reagent which thus may serve as the basis for the catalytic effect. The calculations of Morokuma and Muguruma,[8] e.g., demonstrated that the hydrogen bonding of a single water molecule to the reaction $SO_3 + H_2O \rightarrow H_2SO_4$ lowered the barrier by 25 kcal/mol through the formation of a very stable six-member ring. This catalytic effect was found to be consistent with the gas phase SO_3 hydration experiments of Molina and co-workers[16] and Lovejoy et al.[17] Tao and co-workers[6] found that further solvation of the SO_3 in larger clusters led to even lower TS barriers which seemed to converge for large clusters which might be regarded as the solution limit. Vohringer-Martinez et al.[18] have recently established the occurrence of water catalysis for the bimolecular $OH + CH_3CHO \rightarrow H_2O + CH_3CO^•$ reaction. Clustering with a single water molecule was again found to significantly lower the barrier to hydrogen abstraction. Phillips and co-workers[7] likewise noted that the addition of 1−4 water molecules dramatically lowered the barrier for the dechlorination reaction $CH_2(OH)Cl \rightarrow CH_2O + HCl$. In a preliminary work to the present study,[19] we

have found that the TS for the defluorination reaction $CH_2(OH)F \rightarrow CH_2O + HF$ is strongly stabilized through the formation of stable 6-member rings (one H_2O), 8-member rings (two H_2O's), or 10-member rings (three H_2O's). The possibility of water catalysis being effective in small water clusters in the gas phase would have important consequences for atmospheric chemistry.[20−22]

For thermally activated reactions, a substantial lowering of the TS barrier by hydrogen bonding is expected to accelerate the rate of reaction. Using transition state theory (TST), the rate coefficient in the presence of water is approximated by

$$k(T) = \kappa(T) \frac{k_B T}{h} \exp(-\Delta G/k_B T) \qquad (1)$$

where $\kappa(T)$ is a modest transmission coefficient that takes into account dynamical effects of the solvent.[23] The free energy of activation, ΔG, strongly correlates with the barrier height, ΔE^{TS}, and thus a quantum chemical determination of the barrier energies should provide a reliable gauge of catalytic behavior. However, under more general "nonthermal" conditions, the effect of dynamics may play an important role in the reaction and could possibly alter the catalytic behavior.

In this work we examine the possibility of water catalysis for photochemical reactions occurring on the ground electronic surface. Excitation energies required for reaction generally exceed that of the fundamental vibrational transitions, and thus the excited reagent is produced by (1) vibrational overtone excitation, (2) spontaneous internal conversion, or (3) stimulated emission pumping.[24,25] In any of these excitation processes, the photon energy is deposited "locally" into one or several vibrational modes, and reaction occurs when the energy flows into the reaction coordinate. While the ground state barrier is lowered by hydrogen bonding, the nonequilibrium distribution of the excitation energy creates the possibility that (nonstatistical) dynamical effects[26] may play an important role, perhaps even suppressing the catalytic enhancement. To understand the photochemical process and the differences from the thermal counterpart, we study the dynamics of the vibrational overtone induced reaction in the hydrated clusters

$$CH_2(OH)F{\cdot}(H_2O)_n + h\nu \rightarrow CH_2O + HF{\cdot}(H_2O)_n \qquad (i)$$
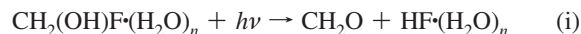
The photon excites the OH-stretching local mode that is known to be a strong chromophore for overtone excitation. Since the barrier energy is significantly higher than the hydrogen bonding energy (ΔE^{EVAP}), reaction (i) must be viewed in competition with the evaporation process.
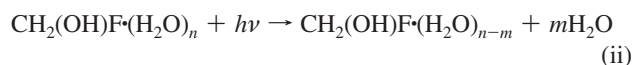
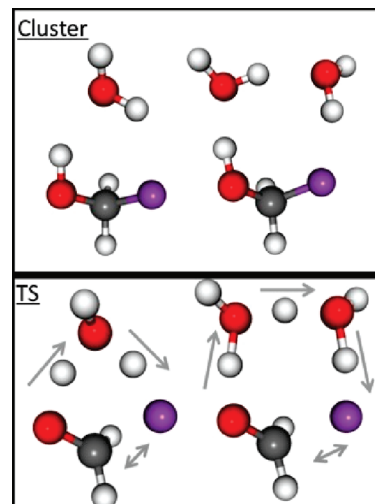$$CH_2(OH)F{\cdot}(H_2O)_n + h\nu \rightarrow CH_2(OH)F{\cdot}(H_2O)_{n-m} + mH_2O \qquad (ii)$$
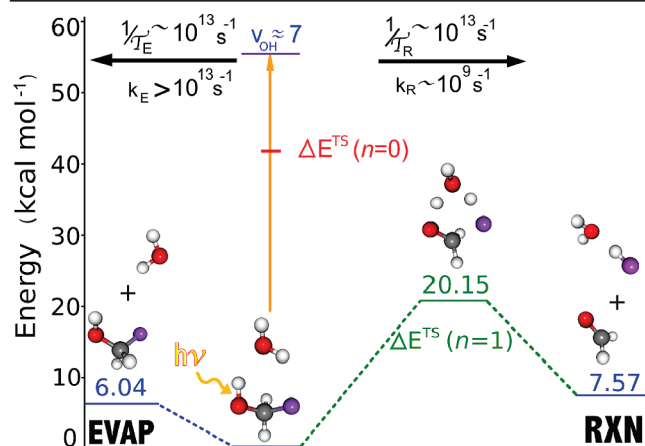
Figure 1. Schematic diagram illustrating the reactive HF elimination and evaporative processes for the monohydrate fluoromethanol.


Figure 2. Equilibrium and transition state geometries obtained at the B3LYP/6-31+G(d,p) level.

Table 1. Energetic Characteristics of Reactions Obtained Using B3LYP/6-31+G(d,p) with Zero-Point Corrections (kcal/mol)

Species	TS Barrier	Evaporation Threshold	Endothermicity, ΔE
CH$_2$FOH	40.50		9.14
CH$_2$FOH(H$_2$O)	20.15	6.04	7.62
CH$_2$FOH(H$_2$O)$_2$	15.28	15.37	9.48

Process (ii) represents irreversible energy flow out of the reactive system that generally leaves the cluster energy below the barrier and hence quenches reaction (i). Since $\Delta E^{TS} > \Delta E^{EVAP}$, we expect that if the excitation energy were to randomize quickly within the cluster, then the lower barrier process (ii) would dominate over process (i) and the reaction would be effectively suppressed. Thus, reaction (i) should occur with an appreciable rate only if the dynamics is "direct", i.e. nonstatistical, and occurs on a time scale commensurate with or faster than that of the energy transfer process, $\tau_{ET} \geq \tau_R$. Such time scale restrictions are not expected to apply to thermally induced reactions in solution or cluster phase where (ii) is reversible and a near-equilibrium distribution of reagent states is maintained.

Since the photoactivated reagents must lie in a highly nonequilibrium distribution for the chemical reaction to occur at all, we do not expect TST rate expressions to apply. Thus, we cannot simply rely on the energetics of the TS to determine whether or not the water catalytic effect occurs in a photochemical reaction. Instead, we must model the dynamics of the reactive process from reagents to products. In the remainder of this work, we describe and analyze dynamical simulations that we have carried out for reactions in finite water clusters. The specific objective of the calculations is to obtain the quantum yield for the reaction as a function of excitation energy, $\Phi(E = h\nu)$. For an isolated gas phase molecule CH$_2$(OH)F ($n = 0$ in i), the energy dissipation channel is absent and we should observe a threshold, $\Phi(E) \approx \theta(E - \Delta E^{TS}(n = 0))$, in the absence of quantum tunneling. Here θ is the Heaviside step function and $\Delta E^{TS}(n = 0)$ is the "uncatalyzed" reaction barrier in the absence of water. Of course the time scale for reaction is potentially longer than typical gas phase collision times in this hypothetical case. For hydrated clusters with $n \neq 0$, we shall judge the photochemical process to be water catalyzed if we observe the threshold in $\Phi(E)$ to be shifted in energy to a value significantly below $\Delta E^{TS}(n = 0)$. In an ideal limit, the threshold might move all the way to the hydrated barrier position. It is also possible to observe anticatalysis, where the threshold for the cluster reaction lies above the TS of the bare, i.e. $n = 0$, reaction.

In Figure 1 we present a schematic diagram that illustrates the competition between reaction and dissipative-evaporation processes. Shown is the case of the monohydrate cluster excited to the alcohol OH($v \approx 7$) level with $h\nu = 57$ kcal/mol. Using microcanonical Rice−Ramsperger−Kassel−Marcus (RRKM) theory, the statistical reaction rate, k_R, is seen to be over 4 orders of magnitude smaller than the evaporation rate, k_E. On the other hand, the dynamical simulations (discussed below) show a reaction "rate" that is actually

comparable to the evaporation rate. We note that the direct reaction occurs on a time scale roughly 10^4 times faster than that predicted by statistical theory.

We have performed an extensive set of *ab initio* dynamics simulations at a series of excitation energies for the $n = 1$ and $n = 2$ clusters pictured in Figure 2 where we have used the B3LYP/6-31+G(d,p)[27] method implemented with the Gaussian03 package.[28] We have demonstrated that this level of theory gives fairly reasonable values for binding and TS energies, geometries, and spectroscopic properties,[29] yet is sufficiently inexpensive to permit large scale dynamical simulations. Since our purpose is to illustrate generic dynamical behavior rather than to model specific experiments, we believe that the DFT calculations are adequate here. The methodological details of the calculations have been presented previously[19] and here are only briefly reviewed. The initial states of the clusters were taken to be the ro-vibrational ground state of the most stable isomer, i.e. $T = 0$ K and $J = 0$, and are characterized in Figure 2 and Table 1. In a previous study[30] of overtone excitation of glyoxylic acid, it was found that the energy relaxation rate of the OH-chromophore was insensitive to temperature. The *ab initio* dynamics simulations are performed using the variable step size Hessian based predictor-corrector integrator. The zero-point energy of the ground state of the cluster was included using normal mode sampling for all vibrational degrees of freedom. The one-dimensional OH-stretching potential was numerically generated from B3LYP/6-31+G(d,p) for each trajectory in the initial ensemble. The OH-local mode coordinate and velocity were selected to correspond to the desired excitation energy with a random vibrational phase. The velocities were scaled so that every trajectory in the ensemble had exactly the same total energy. Each trajectory is propagated until (1) the distance between the centers of mass of the fluoromethanol and a water molecule becomes greater than 8.5 a$_0$, (2) the center of mass separation of HF and CH$_2$O becomes greater than 8.5 a$_0$, or (3) the time of propagation becomes long and the excitation energy dissipates from the OH-chromophore. Care was taken to verify that nonreactive trajectories that satisfied the stopping criteria would
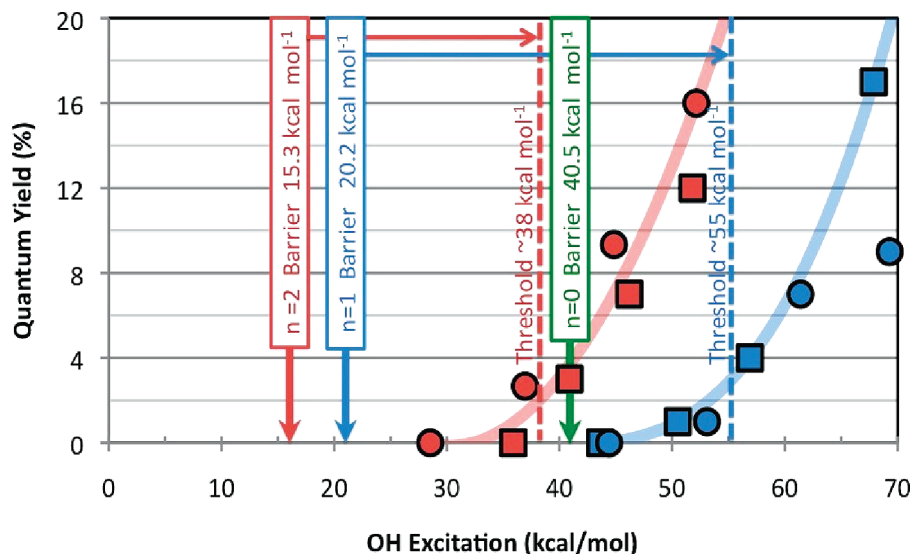
Figure 3. Quantum yield, the fraction of reactive trajectories, versus photon energy for mono- (blue curve) and di- (red curve) clusters obtained from *ab initio* dynamics simulations with $T = 0$ K and $J = 0$. The circles (squares) represent alcohol (water) OH excitation.

not have reacted. Batches of 75−200 *ab initio* trajectories were run for the monohydrate and dihydrate clusters to simulate OH-stretch excitations over the range $\Delta v = 3-9$, which corresponds roughly to energies 30−70 kcal/mol above the zero-point. Two possible chromophores were investigated: (1) the alcohol OH-group and (2) the water OH-group hydrogen bonded to the F-atom.

The main results of this work are displayed in Figure 3 that depicts the quantum yield versus excitation energy. A dramatic delayed threshold effect is clearly apparent in the results where the reaction is not observed until the excitation energy lies far above the hydrated TS energy. Consider first the monohydrate cluster shown with blue symbols (squares for alcohol excitation and circles for water excitation). For both chromophores of the monohydrate, the phenomenological reaction threshold does not occur until the photon energy is above 50 kcal/mol which is significantly more than the bare $CH_2(OH)F$ TS at 40 kcal/mol. The results for the two chromophores are nearly equal near the threshold, but significant mode specificity develops at higher excitations where the alcohol excitation is more effective promoting reaction. The dihydrate results are similar to those for the monohydrate except they are shifted downward, and the mode specificity has mostly disappeared. The threshold for the reaction of $n = 2$ occurs at roughly 38 kcal/mol for both chromophores. Thus, the classical threshold is only 1−2 kcal/mol below the bare TS energy. Hence, due to the delayed threshold behavior we see an anticatalytic effect for the $n = 1$ case and essentially no catalysis for the $n = 2$ case. Naturally, the modest sample size of the *ab initio* trajectories makes it impossible to determine if very small but nonzero quantum yields (i.e., $0.01 > \Phi$) occur at the low excitation energies, but the existence of a pronounced delayed threshold does seem apparent from the results.

Abstractly, the physical origin of the delayed threshold effect is completely understandable in terms of time scales. Because the irreversible water evaporation process is in competition with and quenches the reactive process, photoexcited clusters will tend to evaporate before the dynamics can "find" the low energy TS which requires roughly the statistical lifetime. On the short time scale set by evaporation, the reactive trajectories must cross to products at an unfavorable (higher energy) location of the potential energy surface far from the TS. This stands in contrast to thermally activated reactions where water evaporation is reversible and does not quench the reaction. In that case, the clusters may decay and recondense many times on the time scale of the reaction.

To more fully appreciate the reaction dynamics and the origin of the delayed threshold effect, we plot several ensemble averaged time dependent quantities in Figure 4. In the upper panels, we show the "cumulative event probability" for reaction versus time. A reaction time is determined for each of the N_R reactive trajectories based on a distance criterion. Then the cumulative event probability is given by $\sum_i^{N_R} \theta(t - \tau_i)/N_R$ which tends toward 1 as $t \rightarrow \infty$. Likewise, a cumulative event probability for evaporation is defined from the N_E evaporative trajectories and is shown in the lower panels of Figure 4. It is clear that the time scale for reaction is quite short, ∼70 fs, and is not strongly dependent upon the level of excitation. The time scale for evaporation is somewhat longer, ∼100 fs, and shows little energy dependence. The results are clearly consistent with a nonstatistical direct reaction since the reaction process is effectively over before significant energy randomization takes place. Indeed, if trajectories did not react quickly, <200 fs, no reaction would be observed regardless of the propagation time. For comparison, the reaction and evaporation rates were also computed using microcanonical RRKM theory. As expected, the statistical reaction rates were dramatically lower than dynamical rates with the evaporation rate dominating over the reaction. At $\Delta E = 57$ kcal/mol for $n = 1$, e.g., RRKM theory predicts $k_{Rxn} \approx 10^9$ s^{-1} and $k_{Evap} \geq 10^{13}$ s^{-1} while dynamical simulation reveals both rates are near 10^{13} s^{-1}.

Since the photochemical reaction is clearly nonstatistical, it is interesting to contrast the reaction mechanism suggested by the intrinsic reaction path from the potential to that actually observed in the dynamics. The intrinsic reaction paths emanating from the saddlepoints depicted in Figure 2 have been computed for the $n = 1$ and $n = 2$ clusters. Along the reaction path, the two (for $n = 1$) or three (for $n = 2$) hydrogen atoms within the ring are transferred nearly simultaneously. This low energy pathway is a concerted multiple H-atom transfer process. Furthermore, the ring structure at the TS is significantly compressed relative to the equilibrium cluster geometry and the reaction is initiated by the excitation of the low frequency ring breathing mode. A close inspection of the actual trajectories reveals that the true dynamics is quite different. Following the OH-excitation, the H-atom tends to undergo a high frequency chattering motion[31,32] back and forth between neighboring O-atoms in the ring as the H-atom is delocalized.[33] For a reactive trajectory, the H-atom becomes fixed to the acceptor O-atom and a sequence of distinct (nonconcerted) H-atom transfers ensues. Furthermore, it is found that the excitation
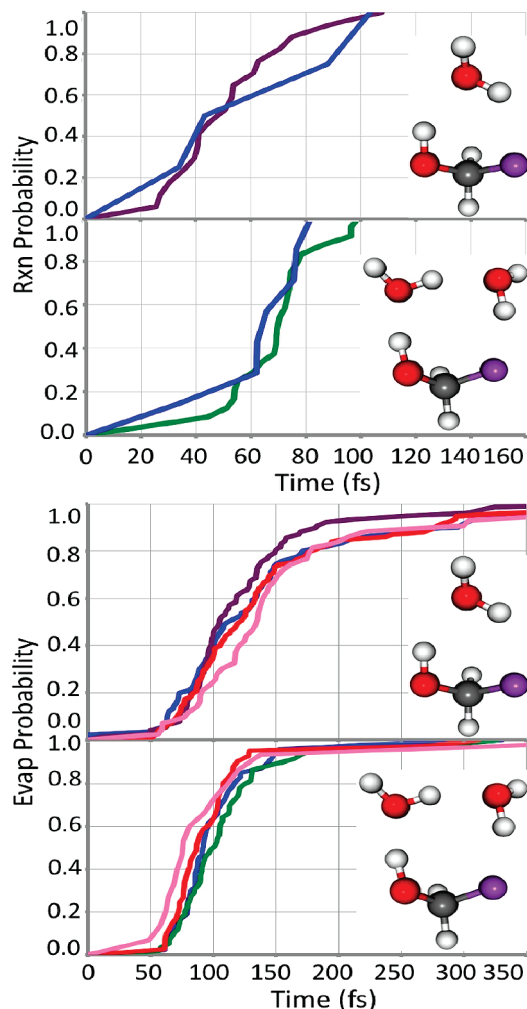
Figure 4. Cumulative event probability for reaction and evaporation versus time for the $v = 9$ (violet), $v = 8$ (green), $v = 7$ (blue), $v = 6$ (red), and $v = 5$ (pink) overtone excitations on the $n = 1$ and $n = 2$ clusters.

of the low frequency ring mode occurs in the final stages of the reaction dynamics and does not follow the intrinsic reaction path. Since the true dynamical barrier passage problem takes place so far from the low energy TS, it should be expected that a significantly higher minimum level of excitation than ΔE^{TS} is required for reaction.

Several conclusions can be drawn from this work. First and foremost, a quantum chemistry prediction of a TS barrier lowering through hydrogen bonding with water is insufficient to establish the existence of water catalysis for some photochemical reactions. The competition between evaporation and reaction must often be modeled dynamically because of the irreversible and nonequilibrium character of the photochemical processes of reaction and evaporation. Second, it is clear from Figure 3 that there is a strong effect on $\Phi(E)$ and other dynamical quantities due to the number of clustering water molecules. Indeed, the difference in the threshold energy for $n = 1$ and $n = 2$ is about 13 kcal/mol which is even larger than difference between $\Delta E^{TS}(n = 2)$ and $\Delta E^{TS}(n = 1)$. It would be interesting to model the dynamics in larger clusters to address the issue of whether water catalysis may occur in the solution limit of $n \rightarrow \infty$. Of course for a very large water cluster the notion of evaporation is replaced with the related process of irreversible intermolecular energy transfer.[34] We have carried out several preliminary calculations with $n = 3$ (see Supporting Information) which do not appear to show very much difference

from the $n = 2$ case; however the question remains open in lieu of more extensive calculations. We note that the pronounced shift in threshold position with cluster size opens the possibility of photochemical size selectivity in atmospheric processes where distributions of cluster sizes are known to occur. Finally, while the limitations of the present methods that employed classical mechanics and DFT will likely result in some quantitative error, we believe the generic delayed threshold behavior observed here would also exist in more realistic simulations.

Supporting Information Available: Further details of the dynamical simulations, RRKM results, product energy distributions, reaction event probablilities, $n = 3$ results, and complete ref 28 are presented. This material is available free of charge via the Internet at http://pubs.acs.org.

References

(1) Rideout, D. C.; Breslow, R. *J. Am. Chem. Soc.* **1980**, *102*, 7816.
(2) Breslow, R. *Acc. Chem. Res.* **1991**, *24*, 159.
(3) Chandrasekhar, J.; Shariffskul, S.; Jorgensen, W. L. *J. Phys. Chem. B* **2002**, *106*, 8078.
(4) Li, C. J. *Chem. Rev.* **1993**, *93*, 2023.
(5) Staikova, M.; Oh, M.; Donaldson, D. J. *J. Phys. Chem. A* **2005**, *109*, 597.
(6) Larson, L. J.; Kuno, M.; Tao, F.-M. *J. Chem. Phys.* **2000**, *112*, 8830–8838.
(7) Phillips, D. L.; Zhao, C.; Wang, D. *J. Phys. Chem. A* **2005**, *109*, 9653.
(8) Morokuma, K.; Muguruma, C. *J. Am. Chem. Soc.* **1994**, *116*, 10316.
(9) Xu, X.; Muller, R. P.; Goddard, W. A., III. *Proc. Natl. Acad. Sci. U.S.A.* **2002**, *99*, 3376.
(10) Deng, C.; Wu, X. P.; Sun, X. M.; Ren, Y.; Sheng, Y. H. *J. Comput. Chem.* **2008**, *30*, 285.
(11) Jorgensen, S.; Kjaergaard, H. G. *J. Phys. Chem. A* **2010**, *114*, 4857.
(12) Eigen, M. *Discuss. Faraday Soc.* **1965**, *39*, 7.
(13) Bell, R. P.; Millington, J. P.; Pink, J. M. *Proc. R. Soc. London, Ser. A* **1968**, *303*, 1.
(14) Cabani, S.; Gianni, P.; Matteoli, E. *J. Phys. Chem.* **1972**, *76*, 2959.
(15) Yamabe, T.; Yamashita, K.; Kaminoyama, M.; Koizumi, M.; Tachibana, A.; Fukui, K. *J. Phys. Chem.* **1984**, *88*, 1459.
(16) Janye, J. T.; Poschl, U.; Chen, Y.-M.; Dai, D.; Molina, L. T.; Worsnop, D. R.; Kolb, C. E.; Molina, M. J. *J. Phys. Chem.* **1997**, *101*, 10000.
(17) Lovejoy, E. R.; Hanson, D. R.; Huey, L. G. *J. Phys. Chem.* **1996**, *100*, 19911.
(18) Vohringer-Martinez, E.; Hansmann, B.; Hernandez, H.; Francisco, J. S.; Troe, J.; Abel, B. *Science* **2007**, *315*, 497.
(19) Takahashi, K.; Kramer, Z. C.; Vaida, V.; Skodje, R. T. *Phys. Chem. Chem. Phys.* **2007**, *9*, 3864.
(20) Vaida, V.; Headrick, J. E. *J. Phys. Chem. A* **2000**, *104*, 5401. Vaida, V. *J. Phys. Chem. A* **2009**, *113*, 5.
(21) Aloisio, S.; Francisco, J. S. *Acc. Chem. Res.* **2000**, *33*, 825.
(22) Njegic, B.; Raff, J. D.; Finlayson-Pitts, B. J.; Gordon, M. S.; Gerber, R. B. *J. Phys. Chem. A* **2010**, *114*, 4609.
(23) Truhlar, D. G.; Hase, W. L.; Hynes, J. T. *J. Phys. Chem.* **1983**, *87*, 2664.
(24) Crim, F. F. *Science* **1990**, *249*, 1387.
(25) Konen, I. M.; Li, E. X. J.; Stephenson, T. A.; Lester, M. I. *J. Chem. Phys.* **2005**, *123*, 204318.
(26) Lourderaj, U.; Hase, W. L. *J. Phys. Chem. A* **2009**, *113*, 2236.
(27) Becke, A. D. *J. Chem. Phys.* **1992**, *98*, 5648. Lee, C.; Yang, W.; Parr, R. G. *Phys. Rev. B* **1988**, *37*, 785. Hehre, W. J.; Ditchfield, R.; Pople, J. A. *J. Chem. Phys.* **1971**, *56*, 2257. McLean, A. D.; Chandler, G. S. *J. Chem. Phys.* **1980**, *72*, 5639. Clark, T.; Chandrasekhar, J.; Spitznagel, G. W.; Schleyer, P. V. *J. Comput. Chem.* **1983**, *4*, 294–301. Hariharan, P. C.; Pople, J. A. *Theor. Chim. Acta* **1973**, *28*, 213. Francl, M. M.; Petro, W. J.; Hehre, W. J.; Binkley, J. S.; Gordon, M. S.; DeFrees, D. J.; Pople, J. A. *J. Chem. Phys.* **1982**, *77*, 3654.
(28) Frisch, M. J. *Gaussian 03*, revision C.02; Gaussian, Inc.: Wallingford, CT, 2004.
(29) Havey, D. K.; Feierabend, K. J.; Takahashi, K.; Skodje, R. T.; Vaida, V. *J. Phys. Chem. A* **2006**, *110*, 6439.
(30) Takahashi, K.; Plath, K. L.; Axson, J. L.; Nelson, G. C.; Skodje, R. T.; Vaida, V. *J. Chem. Phys.* **2010**, *132*, 094305.
(31) Skodje, R. T. *Annu. Rev. Phys. Chem.* **1993**, *44*, 145.
(32) Takahashi, K.; Plath, K. L.; Skodje, R. T.; Vaida, V. *J. Phys. Chem. A* **2008**, *112*, 7321.
(33) Miller, Y.; Gerber, R. B. *J. Am. Chem. Soc.* **2006**, *128*, 9594.
(34) Elles, C. G.; Crim, F. F. *Annu. Rev. Phys. Chem.* **2006**, *57*, 273.

JA107335T